Infragravity waves on the continental shelf

Evangelidis, Dimitrios

Monterey, California. Naval Postgraduate School

NAVAL POSTGRADUATE SCHOOL
MONTEREY, CALIFORNIA

THESIS

INFRAGRAVITY WAVES ON THE CONTINENTAL SHELF

by

Dimitrios A. Evangelidis

June, 1996

Thesis Advisor: Thomas H.C. Herbers
Second Reader: Edward B. Thornton

Approved for public release; distribution is unlimited.

REPORT DOCUMENTATION PAGE	Form Approved OMB No. 0704-0188

1. AGENCY USE ONLY *(Leave blank)*	2. REPORT DATE June 1996	3.REPORT TYPE AND DATES COVERED Master's Thesis

4. TITLE AND SUBTITLE Infragravity Waves on the Continental Shelf	5. FUNDING NUMBERS
6. AUTHOR(S) Dimitrios A. Evangelidis	
7. PERFORMING ORGANIZATION NAME(S) AND ADDRESS(ES) Naval Postgraduate School Monterey CA 93943-5000	8. PERFORMING ORGANIZATION REPORT NUMBER
9. SPONSORING/MONITORING AGENCY NAME(S) AND ADDRESS(ES) Office of Naval Research	10. SPONSORING/MONITORING AGENCY REPORT NUMBER
11. SUPPLEMENTARY NOTES The views expressed in this thesis are those of the author and do not reflect the official policy or position of the Department of Defense or the U.S. Government.	
12a. DISTRIBUTION/AVAILABILITY STATEMENT Approved for public release; distribution is unlimited.	12b. DISTRIBUTION CODE

13. ABSTRACT *(maximum 200 words)*

The variability of infragravity-frequency (0.004-0.04 Hz) motions on a wide continental shelf was examined with data from a 100km-long transect of bottom pressure recorders extending from the beach (6m depth) to the shelf break (87m depth) near Duck, North Carolina. The observed infragravity motions are a mixture of forced waves, phase-coupled to local wave groups, and (uncoupled) free waves. Although the contribution of forced waves to the infragravity energy increases with both increasing swell energy and decreasing water depth, the shelf is usually dominated by free waves. The observed free waves are predominantly radiated from nearby beaches. The strong attenuation of infragravity waves observed across the inner shelf is primarily the result of refractive trapping and is well described by a WKB model. Across the flatter, irregular outer shelf the observed attenuation is weaker but increases with increasing swell energy, suggesting that significant damping occurs on the shelf during storms, consistent with earlier studies. At the deepest instrumented sites, weaker correlations between infragravity and swell energy levels, and weaker depth dependence of infragravity energy levels are observed, suggesting that remotely generated waves are important seaward of the shelf break.

14. SUBJECT TERMS Infragravity waves, surf beat, continental shelf, ocean surface waves	15. NUMBER OF PAGES 54
	16. PRICE CODE

17. SECURITY CLASSIFICATION OF REPORT Unclassified	18. SECURITY CLASSIFICATION OF THIS PAGE Unclassified	19. SECURITY CLASSIFICATION OF ABSTRACT Unclassified	20. LIMITATION OF ABSTRACT UL

NSN 7540-01-280-5500 Standard Form 298 (Rev. 2-89)
Prescribed by ANSI Std. 239-18 298-102

Approved for public release; distribution is unlimited.

INFRAGRAVITY WAVES ON THE CONTINENTAL SHELF

Dimitrios Evangelidis
Lieutenant, Hellenic Navy
B.S., Hellenic Naval Academy, 1987

Submitted in partial fulfillment
of the requirements for the degree of

MASTER OF SCIENCE IN PHYSICAL OCEANOGRAPHY

from the

NAVAL POSTGRADUATE SCHOOL
June 1996

ABSTRACT

The variability of infragravity-frequency (0.004-0.04 Hz) motions on a wide continental shelf was examined with data from a 100km-long transect of bottom pressure recorders extending from the beach (6m depth) to the shelf break (87m depth) near Duck, North Carolina. The observed infragravity motions are a mixture of forced waves, phase-coupled to local wave groups, and (uncoupled) free waves. Although the contribution of forced waves to the infragravity energy increases with both increasing swell energy and decreasing water depth, the shelf is usually dominated by free waves. The observed free waves are predominantly radiated from nearby beaches. The strong attenuation of infragravity waves observed across the inner shelf is primarily the result of refractive trapping and is well described by a WKB model. Across the flatter, irregular outer shelf the observed attenuation is weaker but increases with increasing swell energy, suggesting that significant damping occurs on the shelf during storms, consistent with earlier studies. At the deepest instrumented sites, weaker correlations between infragravity and swell energy levels, and weaker depth dependence of infragravity energy levels are observed, suggesting that remotely generated waves are important seaward of the shelf break.

TABLE OF CONTENTS

LIST OF SYMBOLS

f	frequency
$E\{\ \}$	expected value
$E(f)$	energy density spectrum
$E(\theta)$	directional specrtum
B	bispectrum
B_{ii}	integrated bispectrum
P	pressure
$E_{IG,forced}$	forced infragravity energy
$E_{IG,total}$	total infragravity energy
θ	propagation direction
h	water depth
R	ratio of free infragravity energies

ACKNOWLEDGEMENTS

This research was funded by the Office of Naval Research, Coastal Dynamics Program. I wish to express my sincere appreciation to my advisor, Thomas Herbers, for his guidance and for the countless hours of discussion and instruction which determined the success of this effort. I would like also to thank Prof. Edward Thornton and to extend a special thanks to Paul Jessen for his tireless technical support.

I would like also to extend my deepest gratitude to my wife, Niovi, for supporting my work and for her patience, encouragement and understanding.

I. INTRODUCTION

Infragravity waves with typical periods of about 0.5 to 5 minutes, often dominate wave runup on beaches during storms, excite seiches in small harbors, and are believed to be important to nearshore morphology. Observed wave spectra typically show strong variations in infragravity levels across the continental shelf (Figure 1), with maximum levels close to shore and weak infragravity motions in the open ocean. The physical processes that control this variability are investigated here with data from a cross-shelf transect of bottom pressure recorders.

Previous studies (Okihiro et al.,1992; Elgar et al., 1992; Herbers et al., 1994, 1995a) have shown that infragravity waves on the continental shelf are a mix of forced and free waves (Figure 2a). Forced infragravity waves are locally excited by non-linear wave-wave interactions. Two swell components with slightly different frequencies f and $f+\Delta f$ excite a forced secondary wave with a low (infragravity) frequency Δf (Longuet-Higgins and Stewart 1962; Hasselmann 1962). The observed energy levels of forced infragravity waves are accurately predicted by second-order nonlinear theory (Herbers et al., 1994) but their contribution to the total infragravity energy is generally small (Herbers et al., 1995a).

Free infragravity motions on the continental shelf are either waves radiated from nearby beaches, where they are generated by the strong nonlinearities and/or wave breaking that occur in very shallow water, or remotely generated waves arriving from the open ocean (Figure 2a). Extensive observations on both Pacific and Atlantic continental shelf sites show a strong correlation between infragravity and swell energy levels, suggesting that free infragravity waves are predominantly radiated from the beach [Herbers et al., 1995a; and references therein]. Based on observations by Munk (1949) and Tucker (1950), Longuet-Higgins and Stewart (1962) suggested that as the incident swell are dissipated in the surf zone, the associated forced infragravity waves are released as free waves, reflect from the beach and propagate seaward over the continental shelf. Alternatively, Symonds et al. (1982) suggested that slow oscillations in the wave setup, associated with slow variations of the breakpoint location of groupy incident swell, can drive free infragravity waves. Although observations of the directional properties of infragravity waves radiated from shore are in favorable agreement with Longuet-Higgins and Stewart's hypothesis (Herbers et al 1995b), the role of wave-breaking and associated set-up variations in the infragravity wave generation process is still poorly understood.

As free infragravity waves radiated from shore travel into deeper water, they refract towards increasingly oblique

propagation directions relative to the shoreline (Figure 2b). Depending on the initial propagation direction in shallow water, these waves may either radiate to the open ocean (i.e., leaky waves) or reflect back towards the shore from turning points on the sloping beach and shelf (i.e., trapped waves). Theoretical predictions of nonlinear interactions in shallow water show that directionally narrow swell incident on a beach can drive a directionally broad spectrum of free infragravity waves that are predominantly trapped on the shelf with relatively weak radiation to the open ocean (Herbers et al. 1995b).

Observed infragravity energy levels on the beach, shelf and in the open ocean are qualitatively consistent with strong refractive trapping and a relatively weak leaky component (e.g., Webb et al., 1991; Okihiro et al., 1992; Herbers et al., 1995a). However, when local swell energy levels are high, seaward propagating waves dominate the infragravity band, suggesting that free waves radiated from shore are significantly damped before reaching their turning point on the shelf (Elgar et al., 1994; Herbers et al., 1995).

While infragravity waves radiated from shore are predominantly trapped or dissipated on the shelf, a relatively weak leaky component propagates into deep ocean basins. Webb et al. (1991) show that free infragravity waves observed in the open ocean are the weak background radiation

from distant shores where incident swell and infragravity wave energy levels are high. Distant (trans-oceanic) sources appear to dominate the infragravity wave field on the shelf during extremely calm conditions when the generation of infragravity waves on nearby beaches is relatively weak (Herbers et al., 1995a,b). In contrast to the directional broadening and trapping of waves radiated from shore (Figure 2b), remotely generated waves traveling into shallow water refract towards propagation directions that are perpendicular to the shoreline, causing a directionally narrow, shoreward propagating wave field close to shore (Figure 2c). Upon reflection from the beach these waves may propagate back to the open ocean or (if the shelf is irregular) become trapped on the shelf. Observed directional spectra of infragravity waves on the shelf during low wave conditions are indeed bimodal with narrow peaks in shoreward and seaward directions, in contrast to the broad directional spectra (with significant alongshore propagation) typically observed during high energy conditions (Herbers et al., 1995a).

In this study the propagation of infragravity waves across the continental shelf is examined in more detail using measurements collected offshore of Duck, North Carolina. Ten bottom pressure recorders were deployed along a cross-shelf transect extending from the beach (6m depth) to the shelf break (87 m depth) for 4 months during the fall

of 1994. The field data are described in Chapter II. Estimates of the forced and free wave contributions to the infragravity wave field are presented in Chapter III. In Chapter IV the observed cross-shelf variability of free infragravity wave energy is examined, and the importance of refractive trapping and damping effects is discussed. In Chapter V the observations are compared to predictions of a simple geometrical optics - based (WKB) model for the propagation and trapping of long waves(Herbers et al., 1995a). The results are summarized in Chapter VI. All figures are contained in the Appendix.

II. FIELD DATA

Infragravity motions on the continental shelf are investigated with field data collected offshore of the U.S. Army Corps of Engineers Field Research Facility, Duck, North Carolina, as part of the DUCK94 experiment. Ten bottom-pressure sensors were deployed along a 100-km-long cross-shelf transect that extended from the Duck beach to the shelf break (Figure 3). The three shallowest sites X (6m depth), A (12m), and B(20m) span the nearly plane (slope≈0.005) inner shelf. The next 6 sites (C-H) are roughly equally spaced on the wide, irregular (depths 25-50m) outer shelf, and the deepest site I (depth 87m) is on the steep (slope≈0.1) continental slope (Figure 4).

At each site a self-contained battery-powered, internal-recording instrument package was mounted inside an anchor with a surface mooring (sites A-I) or on a pipe jetted in the beach (site X). The instrument package contained a Setra capacitance-type pressure transducer, a Tattletale microprocessor, and a disk drive for data storage. Pressure data were recorded nearly continuously with a 2 Hz sample rate during the four-month-long (August-November, 1994) deployment. Some malfunctioning data acquisition systems were replaced with a cassette data tape storage system with a reduced sampling scheme (a 137-minute-

long record sampled at 1 Hz every 3 hours). Site B suffered significant data loss during the first two months of the experiment, and the instruments at the shallowest sites X and A failed during Hurricane Gordon on November 18. Additionally, high resolution directional wave data were collected in 8m depth (1 km from shore) with a 250m aperture, 14-element array of pressure gauges (deployed and maintained by the U.S. Army Corps of Engineers).

The analysis is based on 3-hour-long records (137 minutes at some sites where longer records were not available). A pressure spectrum with 0.0005 Hz resolution was obtained from each data record based on the Fourier transforms of detided and tapered 34-minute-long data segments. The pressure spectra were subsequently converted to equivalent sea surface elevation spectra using a linear theory depth correction (the correction is small at infragravity frequencies).

The strong variability of infragravity spectral levels across the shelf is illustrated in Figure 5a with the average value of the ratio between the spectral levels observed at each site and the spectral levels observed at the deepest site I. While the cross-shelf variations in spectral levels is weak (less than a factor of 2) at swell frequencies > 0.07 Hz, a strong, consistent increase in spectral levels with decreasing water depth is observed at infragravity frequencies (0.004-0.04 Hz). The infragravity

spectral levels at the shallowest site X are about a factor 30 larger than those observed at the deepest site I. This increase is qualitatively consistent with both the amplification of forced waves in shallow water and the refractive trapping of free waves radiated from shore, but inconsistent with the weak shoaling amplification ($\propto h^{-1/2}$ for a shelf with straight and parallel depth contours) expected for remotely generated infragravity waves arriving from the open ocean (Herbers et al.,1995a; and references therein). While a strong cross-shore decay of infragravity energy levels is observed on the inner shelf (sites X-D) and at the shelf break (sites H-I), the energy variations are more gradual over the broad mid-shelf region between sites D and H (not shown). These observations suggest that the shelf-wide variability of infragravity waves is primarily controlled by large scale depth variations and not strongly affected by local bottom irregularities. The observed cross-shelf variations in spectral levels appear to be approximately constant across the infragravity band. The fluctuations in relative spectral levels observed at the shallowest sites X and A are the expected standing wave patterns associated with shoreline reflections.

Observed correlation coefficients, between spectral levels at infragravity frequencies and the total swell variance are presented in Figure 5b. Swell variances observed at the inner shelf site C (25m depth) are used

throughout this paper to characterize swell conditions on the shelf because variations in swell energy across the shelf are generally small, the depth attenuation of swell in 25m depth is relatively weak, and the site C instrument functioned reliably throughout the experiment. The strong correlation observed at all sites between infragravity and swell energy levels (correlation coefficients squared are above 0.5 in the frequency range 0.004-0.04 Hz) indicates that the infragravity waves are predominantly locally generated (e.g., forced waves or waves radiated from nearby beaches) and that waves arriving from remote sources are relatively unimportant, consistent with earlier observations (Herbers et al. 1995a). Note however, the somewhat weaker correlation observed at site H and particularly site I that suggests a significant contribution of remotely generated waves near the shelf break.

At all sites the correlations drop rapidly at frequencies above about 0.04 Hz because very low-frequency swells from distant storms are statistically independent of the dominant (frequencies > 0.07 Hz) swells. The correlation coefficients are also small below 0.004 Hz, suggesting that these low frequency motions are not driven by swell, consistent with earlier observations (Herbers et al., 1995a, and references therein).

III. FORCED AND FREE WAVE CONTRIBUTIONS

The contributions of forced and free waves to the observed infragravity motions were estimated using bispectral analysis. The method is based on the fact that forced waves are phase-coupled to local swell, while free waves do not contribute to the bispectrum (Herbers et al. 1994). Analogous to the second-order energy density spectrum E(f),

$$E(f)\,df = 2\mathbf{E}\{dP(f)\,dP(-f)\} \tag{1}$$

the third-order bispectrum $B(f,\Delta f)$ is defined as (Hasselmann et al. 1963) :

$$B(f,\Delta f)\,df\,d\Delta f = 2\mathbf{E}\{dP(f)\,dP(\Delta f)\,dP(-f-\Delta f)\} \tag{2}$$

where $\mathbf{E}\{\ \}$ is the expected value and dP(f) is the Fourier-Stieltjes transform of the pressure time series p(t):

$$p(t) = \int_{-\infty}^{\infty} dP(f) \exp(2\pi i f t) \tag{3}$$

An estimate of the contribution of forced waves to the total infragravity variance (over the frequency range 0.004-0.04 Hz) is obtained by integrating the bispectrum $B(f,\Delta f)$ over all pairs of swell components (frequencies f, $f+\Delta f$) with a difference-frequency (Δf) in the infragravity band (see Herbers et al., 1994 for details).

$$B_{ii} = \frac{2\int d\Delta f \int df\ B(f,\Delta f)}{[2\int d\Delta f \int df\ E(f+\Delta f)E(f)\int d\Delta f\ E(\Delta f)]^{1/2}} \qquad (4)$$

The ratio between the forced and total infragravity energies is approximately given by

$$\frac{E_{IG,forced}}{E_{IG,total}} \approx |B_{ii}|^2 \qquad (5)$$

The phases of the bispectral integral B_{ii} observed at the mid-shelf site E (34m depth) are shown in Figure 6. While the imaginary part of B_{ii} is small and approximately randomly scattered about zero, the real parts include large negative values. Although the statistical uncertainty in these bispectral estimates is considerable, the phases are

generally consistent with the theoretical value of 180^0 for weakly nonlinear waves (Hasselmann, 1962). Similar biphases were observed at the other sites (not shown here) except for the shallowest site X, where small, but systematic deviations from 180^0 were observed that are possibly caused by bottom slope effects (i.e., significant depth variations over a wavelength) or phase-coupling between the incident swell and infragravity waves reflected from the beach.

The estimated ratios of forced to total infragravity energy at sites A (12m depth), E (34m) and I (87m) are shown in Figure 7. The estimated forced fraction of the infragravity energy generally increases with both increasing swell energy and decreasing water depth, similar to the trends reported by Herbers et al. (1995a). However, at all sites (including those not shown in Figure 7) the estimated forced wave contribution to the total infragravity variance is usually less than 20% , indicating that free waves dominate the infragravity band.

IV. FREE WAVE VARIABILITY

Energy levels of free infragravity waves radiated from shore generally decrease with increasing distance from shore owing to both propagation and damping effects. On a gently, monotonically sloping shelf with straight and parallel depth contours h(x), the propagation direction θ of a seaward propagating wave component increases according to Snell's law, in the shallow water approximation:

$$\frac{\sin(\theta(x))}{(gh(x))^{1/2}} = constant \qquad (6)$$

until the turning point is reached where $|\theta| = \pi/2$, and the wave reflects back towards shore. Far from shore, the combined effects of unshoaling, refraction and trapping, result in a directionally isotropic wave field with energy levels that are inversely proportional to the water depth (Herbers et al., 1995a). This h^{-1} depth dependence is stronger than the $h^{-1/2}$ dependence predicted for leaky waves propagating perpendicular to straight and parallel depth contours.

While the cross-shelf energy variations owing to linear propagation effects ((un)shoaling, refraction and trapping)

depend primarily on the directional properties of the waves and the shelf topography, the attenuation owing to dissipation effects (e.g., bottom friction) appears to be a strong function of wave energy levels on the shelf (Elgar et al., 1994; Herbers et al., 1995b).

The importance of both propagation and dissipation effects to the cross-shelf variability of free infragravity waves is illustrated in Figure 8 with estimates of the free wave attenuation over different parts of the shelf. The ratio $R_{A,D}$ between free wave energy estimates (obtained by subtracting the bispectrum-based forced wave energy estimates from the total observed infragravity energy, see Chapter III) at inner shelf sites D (depth h_D=34m) and A (h_A=12m), separated by about 30km, varies between 0.2 and 0.6 (Figure 8a). The majority of the $R_{A,D}$ values are in range 0.2-0.5, roughly comparable to the theoretical value h_A/h_D=0.35 for an isotropic trapped wave field. Higher $R_{A,D}$ values in the range 0.5-0.6, closer to the theoretical value $(h_A/h_D)^{1/2}$=0.6 for leaky waves, are observed only on a few occasions with low swell energy levels. These observations suggest that the infragravity band on the inner shelf is dominated by waves that are radiated from shore and refractively trapped by the sloping sea bed, and that contributions of (leaky) remotely generated waves are significant only with very low swell energy levels, consistent with earlier studies (Herbers et al., 1995 a,b).

A more quantitative analysis of propagation and trapping effects on the inner shelf is presented in Chapter V.

The ratio $R_{D,F}$ between sites F and D, also separated by about 30 km, but in about the same depth (h_D=34m, h_F=32m) varies between 0.6 and 1.2, (Figure 8b). Across this relatively flat middle part of the shelf, propagation and trapping effects are expected to be weak, qualitatively consistent with observed $R_{D,F}$ values close to 1. However, a systematic decrease of the observed $R_{D,F}$ with increasing swell variance suggests that waves propagating seaward over the shelf are significantly damped during high-energy swell conditions, consistent with results of earlier studies (Herbers et al., 1995b).

The ratio $R_{F,H}$ (Figure 8c) between outer shelf sites H (h_H=49m) and F (h_F=32m), separated by about 30km, is typically within the range of 0.5-0.8, with again a noticeable trend of decreasing R with increasing swell energy. The estimates suggest continued attenuation of infragravity waves across the outer shelf owing to both propagation and damping processes.

The ratio $R_{H,I}$ (Figure 8d) between energy levels observed at sites I (h_I=87m) and H(h_H=49m) situated near the shelf break varies between about 0.5-0.7 for high energy swell conditions and 0.6-1.1 for low to moderate swell conditions. Sites I and H are separated by only 6 km, and thus, the attenuation owing to bottom friction is expected

to be weak. The $R_{H,I}$ estimates, consistently larger than the theoretical trapped wave value of 0.56, suggest there are significant contributions of remotely generated (leaky) infragravity waves at the shelf break. Although more energetic waves radiated from shore dominate the infragravity wave field close to shore, these waves are attenuated by trapping and damping, and thus, their energy levels are strongly reduced at the shelf break. Relatively weak, remotely generated waves are usually not significant on the beach and shelf but may dominate the infragravity wave field seaward of the shelf break.

V. PREDICTION OF PROPAGATION AND TRAPPING EFFECTS

To demonstrate that the observed strong decrease of infragravity energy across the inner shelf is primarily the result of refractive trapping, the observations are compared here to a simple WKB-geometrical optics model that describes the transformation of a continuous spectrum of waves on a gently sloping sea bed (Herbers et al., 1995a). In the shallow water WKB approximation, the transformation of the directional spectrum $E(\theta;x)$ over a monotonically sloping seabed with straight and parallel depth contours is given by

$$E(\theta;x) = \frac{h_s}{h(x)} E(\theta_s(\theta,x);x_s) \tag{7}$$

where θ=0 corresponds to offshore propagation, and x_s is a location with depth h_s shoreward of x where the propagation direction θ_s is given by Snell's law

$$\sin(\theta_s(\theta;x)) = (\frac{h_s}{h(x)})^{\frac{1}{2}} \sin\theta \tag{8}$$

Waves traveling seaward or shoreward at x_s with propagation

directions θ_s, within the apertures

$$|\theta_s| < \arcsin[(\frac{h_s}{h(x)})^{\frac{1}{2}}]$$

$$|\theta_s-\pi| < \arcsin[(\frac{h_s}{h(x)})^{\frac{1}{2}}] \quad (9)$$

will reach the offshore distance x while all other components are trapped between x_s and x.

WKB predictions of the transformation of free infragravity waves across the inner shelf were initialized with estimates of the directional spectrum $E(\theta)$ (integrated over the infragravity frequency range), obtained from the 8m depth array with a variational technique (Herbers and Guza, 1990). Two contrasting examples of directional spectrum estimates in 8m depth are shown in Figure 9. The top panel shows an example of remotely generated waves with two narrow peaks at about 20^0 (onshore propagating waves arriving from deep water) and 160^0 (presumably the specular reflection of these waves from shore). The bottom panel shows a more typical broad directional spectrum of waves radiated from shore with significant energy at alongshore propagation directions ($\theta \approx 90^0$).

WKB predictions of $E(\theta)$ were made only at sites

A(h_A=12m) and B(h_B=20m) because this section of the shelf is monotonically sloping with relatively small alongshore depth variations. The directional spectra predicted in 12 and 20m depth are similar in shape but broader than the spectrum observed in 8m depth (e.g., Figure 9), and often nearly isotropic in 20m depth (e.g.,Figure 9b).

The directional spectra were integrated to predict the total free infragravity energy at sites A and B. The observed and predicted ratio $R_{A,B}$ between free infragravity energy at sites B and A are compared in Figure 10 for the period of September 22 to November 17 (when all instruments were operational in 8, 12 and 20m depth). The observed and predicted $R_{A,B}$ are generally in good agreement. Note that during days 274-276, when local swell energy levels were very low and the infragravity band is dominated by leaky (remotely generated) waves (Figure 9a), the decrease in energy between 12 and 20m depth is small ($R_{A,B}\approx 0.8-0.9$). This calm period is followed by a sudden increase in swell energy and decrease in $R_{A,B}$ (to about 0.6), that indicates a transition from remotely generated infragravity waves to waves radiated from shore. A similar transition occurred around day 314, but here the predicted $R_{A,B}$ values are somewhat larger than the observed values. Discrepancies are also noted on days 285-287 when the observed attenuation is slightly stronger ($R_{A,B}\approx 0.4-0.6$) than the predicted attenuation ($R_{A,B}\approx 0.6-0.7$). These differences observed during

a severe nor'easter may be the result of damping of free infragravity waves between sites A and B. However, inaccuracies of $E(\theta)$ estimates (e.g., Herbers and Guza, 1990) may also contribute significant errors in the $R_{A,B}$ predictions. Overall the comparisons presented here show that the observed variations in infragravity energy across the inner shelf are primarily the result of linear propagation and trapping effects and well described by a WKB model.

VI. CONCLUSIONS

Infragravity motions with nominal periods of 0.5-5 minutes are important to a variety of nearshore processes. Previous studies have shown that infragravity motions are a mixture of forced waves locally excited by non-linear wave-wave interactions, free waves radiated from nearby beaches, and remotely generated free waves arriving from the open ocean. The variability of infragravity waves on a wide continental shelf is examined with data from a cross-shelf transect of 10 bottom pressure recorders, extending from the beach (6m depth) at Duck, North Carolina to the shelf break (87m depth).

Bispectral analysis, based on the fact that forced waves are phase-coupled to local swell groups while free waves are un-coupled, was used to estimate the forced and free wave contributions to the total infragravity energy. The phases of the bispectra estimates are shown to be in agreement with second order non-linear wave theory.

As in previous studies, the relative contribution of forced waves to the infragravity energy increases with both increasing swell energy and decreasing water depth, but is usually less than 10% at all instrumented sites. The observed infragravity motions on the shelf are clearly dominated by free waves.

The observed strong correlation between infragravity and swell energy levels, and strong decrease in infragravity energy levels between the beach and the shelf break indicate that free waves radiated from shore generally dominate the infragravity wave field on the shelf.

The strong attenuation of infragravity waves observed across the sloping inner shelf is shown to be caused primarily by the refractive trapping of waves propagating into deeper water, and well described by a WKB model. The weaker attenuation usually observed across the relatively flat, but highly irregular outer shelf indicates that the shelf-wide variability of infragravity waves is not strongly affected by scattering from local bottom irregularities. However the attenuation of infragravity waves across the wide outer shelf region increases with increasing swell energy. This trend cannot be explained by linear propagation effects and suggests significant damping of infragravity waves on the shelf during storms, consistent with earlier studies. Remotely generated (leaky) waves sometimes dominate infragravity motions on the shelf during periods of extremely low swell energy levels when the radiation of infragravity waves from nearby beaches is relatively weak. At the deepest instrumented sites, weaker correlations between infragravity and swell energy levels and weaker depth dependence of infragravity energy levels are observed, suggesting that remotely generated waves are important

seaward of the shelf break, possibly because the more energetic waves radiated from shore are strongly attenuated across the shelf.

APPENDIX

Figure 1. Example of wave spectra observed on the North Carolina shelf (site locations are shown in Figure 3).

Figure 2. (a) Sources of infragravity waves. (b) Ray trajectories of free infragravity waves radiated from shore. (c) Ray trajectories of free infragravity waves arriving from a remote source. Dashed lines indicate depth contours.

Figure 3. Bathymetry of the North Carolina shelf. The dashed line indicates the instrumented transect. The pressure sensor sites are indicated by letters.

Figure 4. Cross section of the instrumented transect (dashed line in Figure 3). The pressure sensor sites are indicated by letters (Site D is 7.5 km south of the transect).

Figure 5. (a) Average ratios between the spectral levels observed at various sites and the spectral levels observed at the deepest site I (87m depth). (b) Observed correlation coefficients squared between the logarithms of spectral levels at infragravity frequencies and the total swell variance at site C (over the frequency range 0.04-0.14Hz).

Figure 6. Imaginary versus real part of the bispectral integral B_{ii} observed at site E.

Figure 7. Estimates of the ratio of forced infragravity energy to the total infragravity energy at sites A, E and I versus swell energy (observed at site C).

Figure 8. Observed ratios of the free infragravity wave variances at sites: (a) D (34m depth) and A (12m), (b) F (32m) and D (34m), (c) H (49m) and F (32m) (d) I (87m) and H (49m), versus the swell variance (observed at site C). Dashed lines indicate the theoretical h^{-1} energy variation of an isotropic trapped wave field on a seabed with straight and parallel depth contours. Dashed-dotted lines indicate the weaker theoretical $h^{-1/2}$ energy variation for leaky waves propagating perpendicular to straight and parallel depth contours.

Figure 9. Directional spectrum of infragravity wave energy $E(\theta)$ (arbitrary units) observed in 8m depth (solid line), predicted in 12m depth (dashed line) and predicted in 20m depth (dashed-dotted line) (a) 2 October 1994 (day 275), (b) 4 October 1994 (day 277).

Figure 10. Top panel: Observed swell variance (at site C, units cm^2). Bottom panel: Observed and predicted ratios $R_{A,B}$ between free infragravity wave energy in 20m and 12m depth.

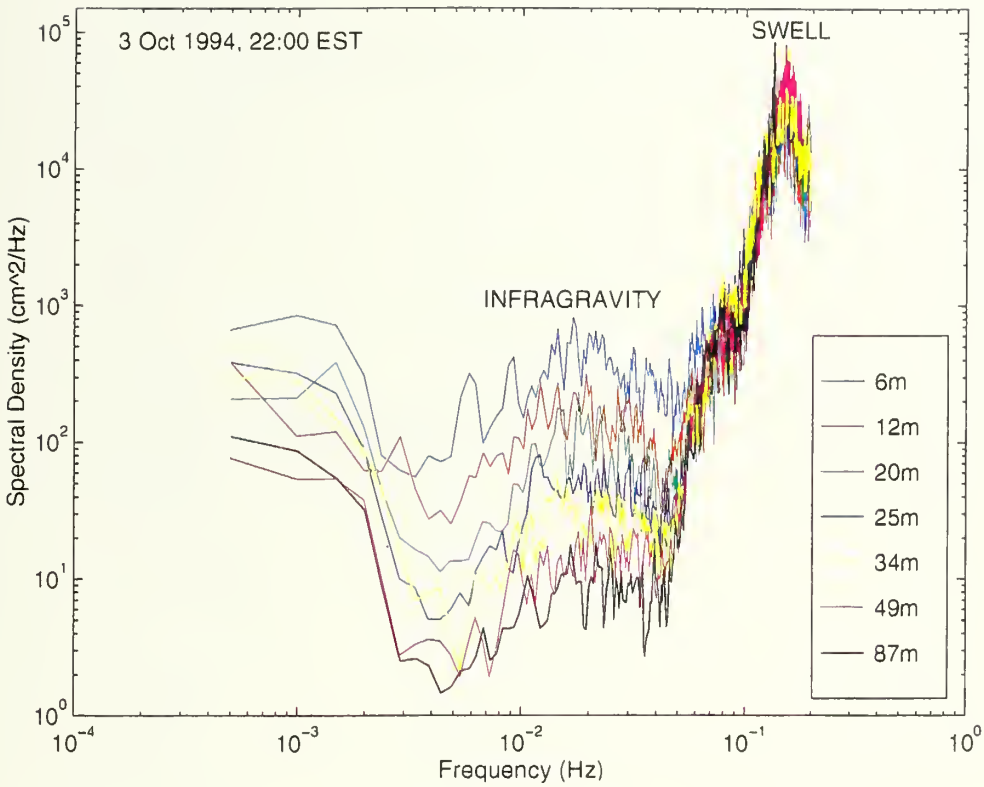
3 Oct 1994, 22:00 EST
SWELL
INFRAGRAVITY
6m
12m
20m
25m
34m
49m
87m
Spectral Density (cm^2/Hz)
Frequency (Hz)
10^5
10^4
10^3
10^2
10^1
10^0
10^{-4}
10^{-3}
10^{-2}
10^{-1}
10^0

Figure 1

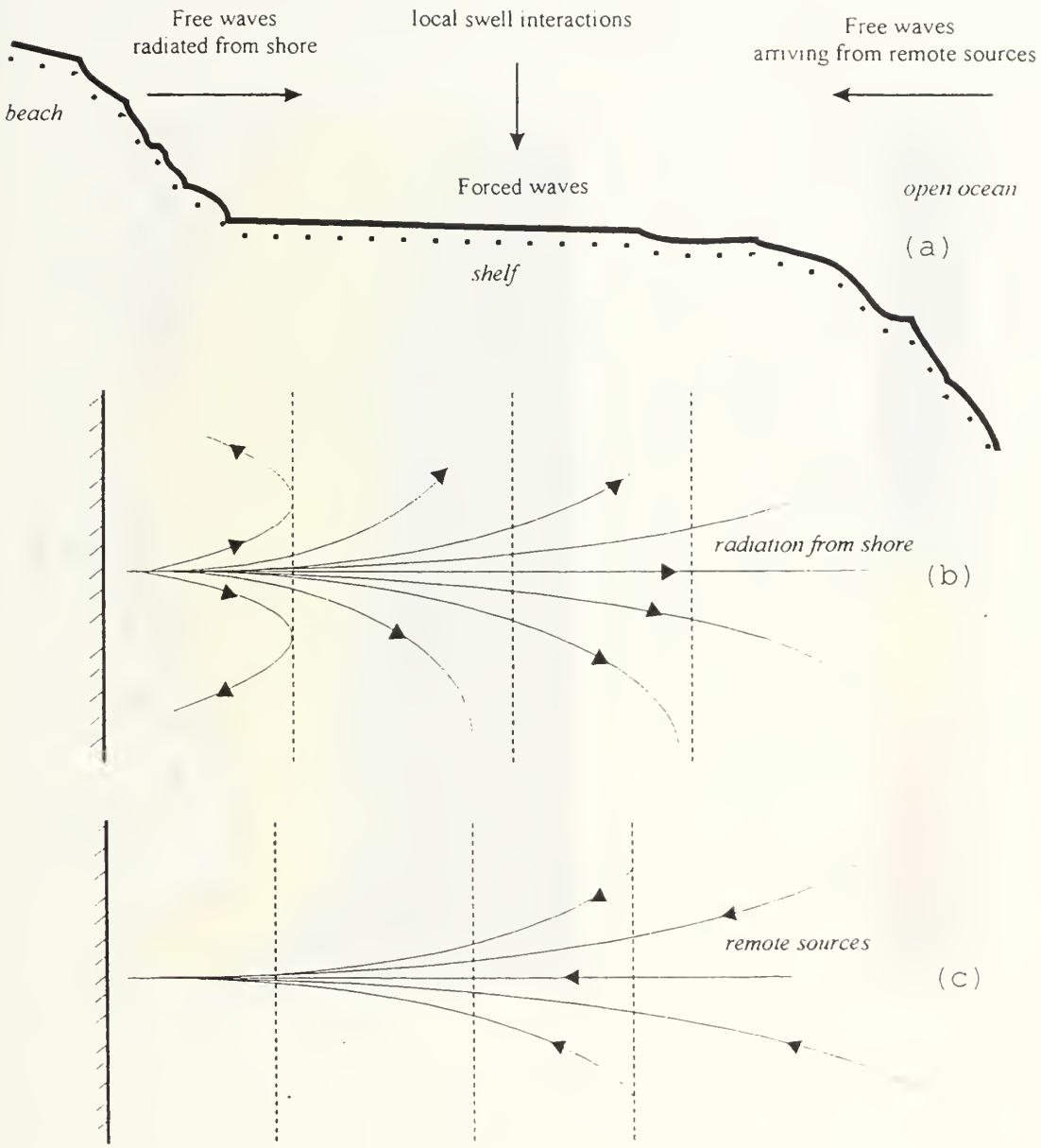
Free waves
radiated from shore
local swell interactions
Free waves
arriving from remote sources
beach
Forced waves
open ocean
(a)
shelf
radiation from shore
(b)
remote sources
(c)

Figure 2

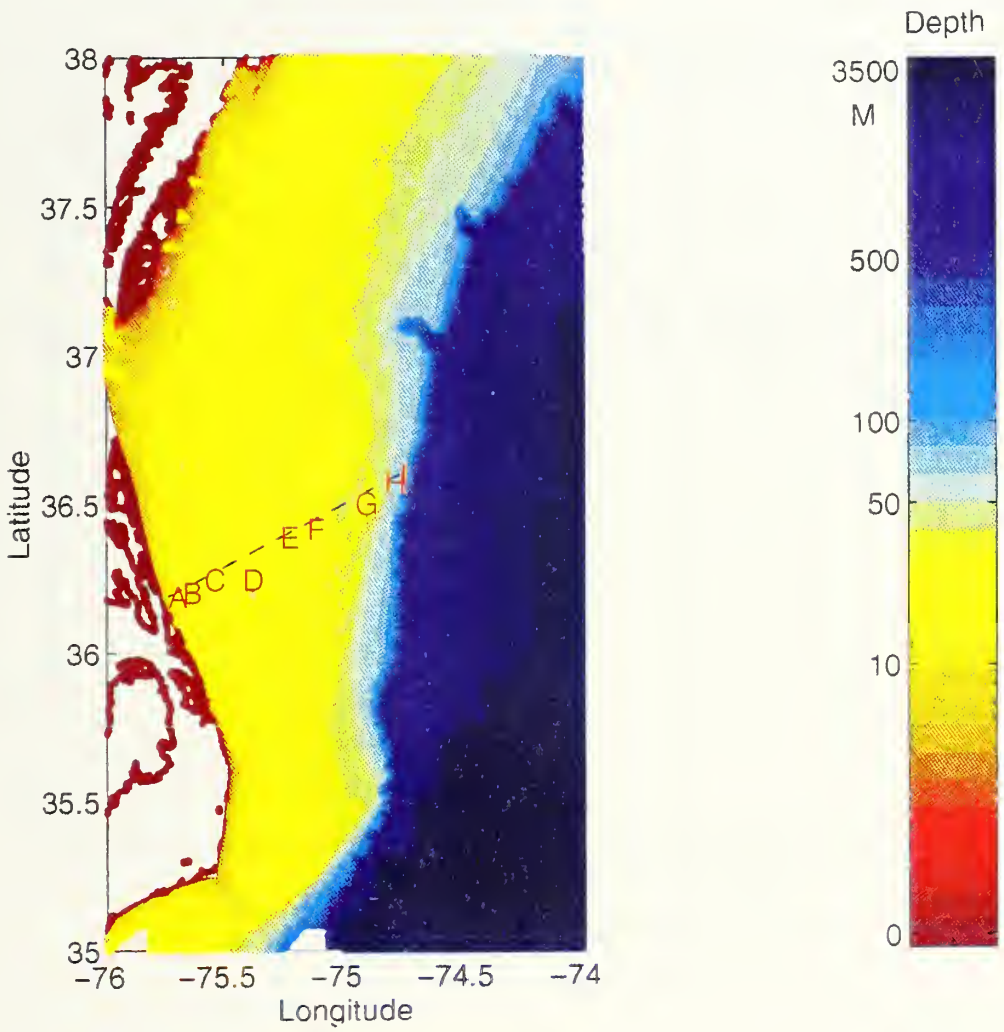
Depth
3500
M
500
100
50
10
0
38
37.5
37
36.5
36
35.5
35
Latitude
−76
−75.5
−75
−74.5
−74
Longitude
A
B
C
D
E
F
G
H

Figure 3

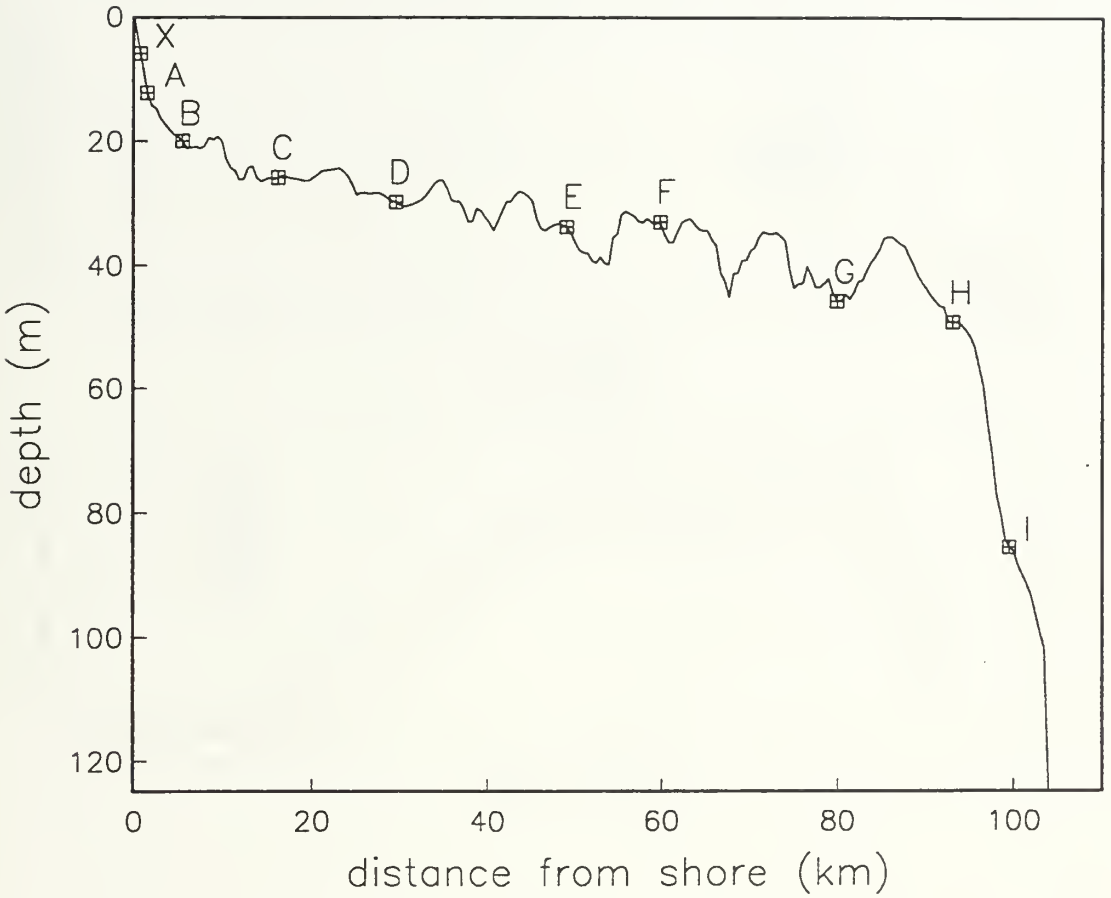
0
20
40
60
80
100
120
depth (m)
X
A
B
C
D
E
F
G
H
I
0
20
40
60
80
100
distance from shore (km)

Figure 4

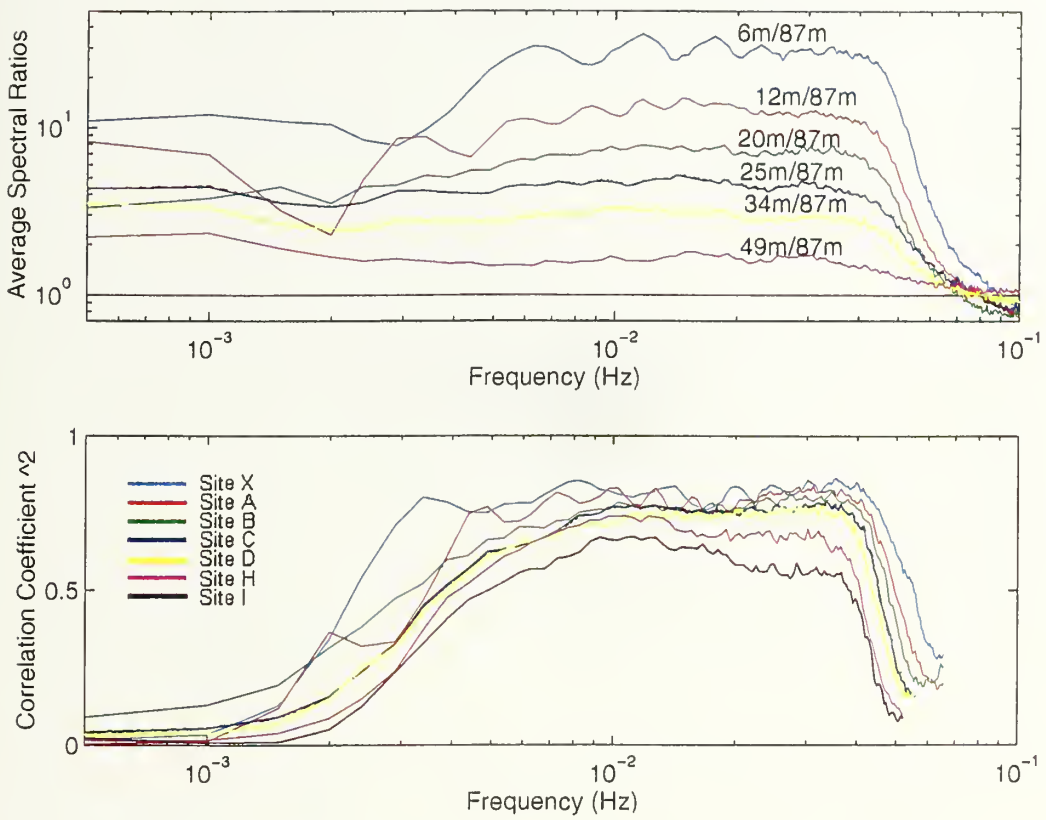
Average Spectral Ratios
10^1
10^0
6m/87m
12m/87m
20m/87m
25m/87m
34m/87m
49m/87m
10^{-3}
10^{-2}
10^{-1}
Frequency (Hz)
Correlation Coefficient ^2
1
0.5
0
Site X
Site A
Site B
Site C
Site D
Site H
Site I
10^{-3}
10^{-2}
10^{-1}
Frequency (Hz)

Figure 5

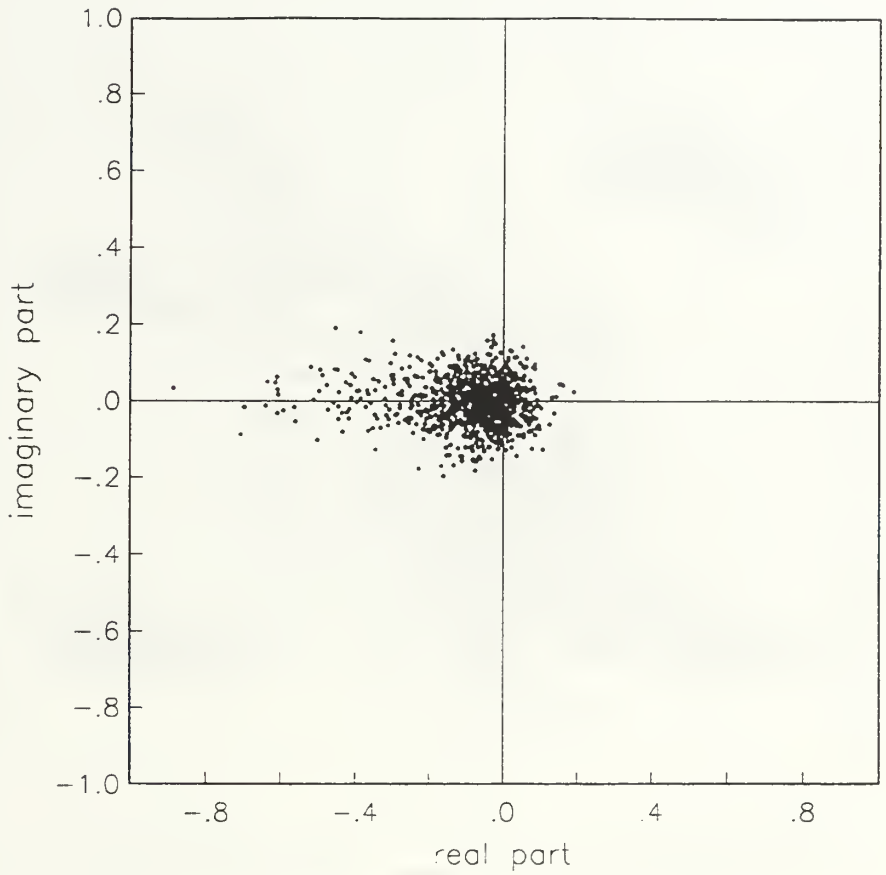

Figure 6

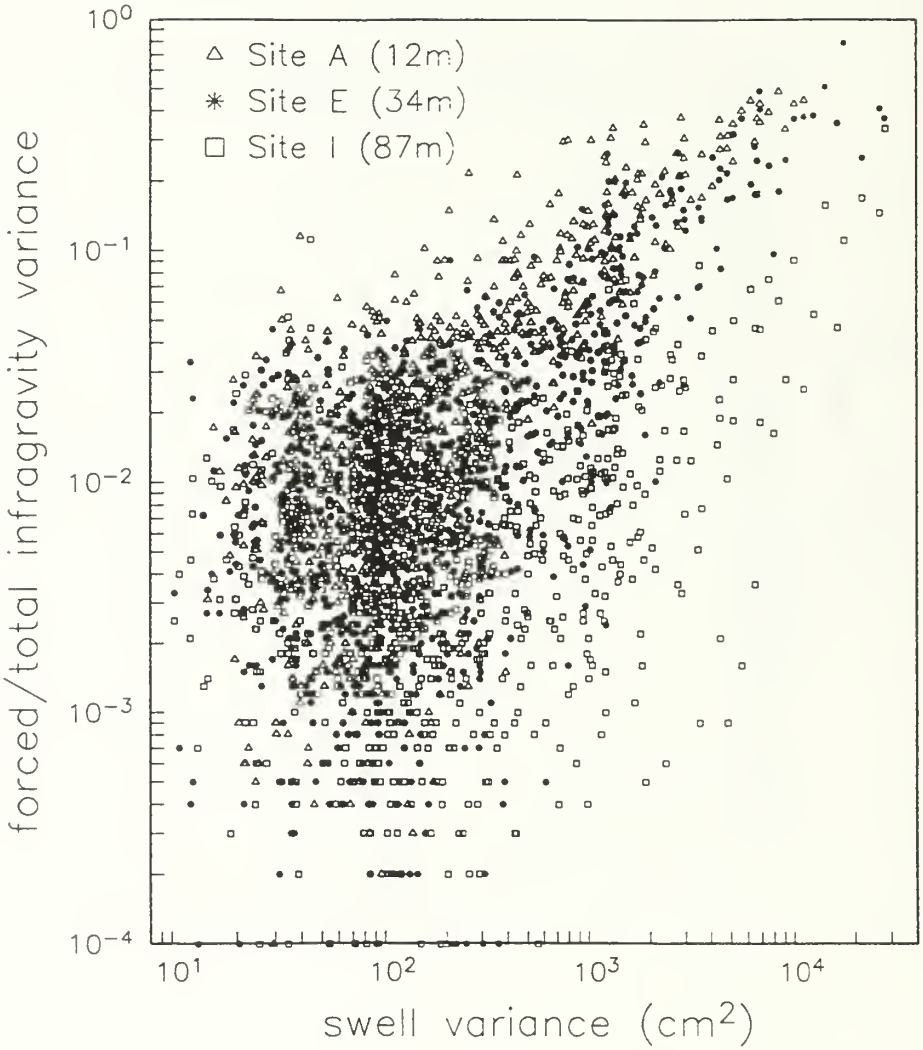
Site A (12m)
Site E (34m)
Site I (87m)
forced/total infragravity variance
swell variance (cm²)
10⁰
10⁻¹
10⁻²
10⁻³
10⁻⁴
10¹
10²
10³
10⁴

Figure 7

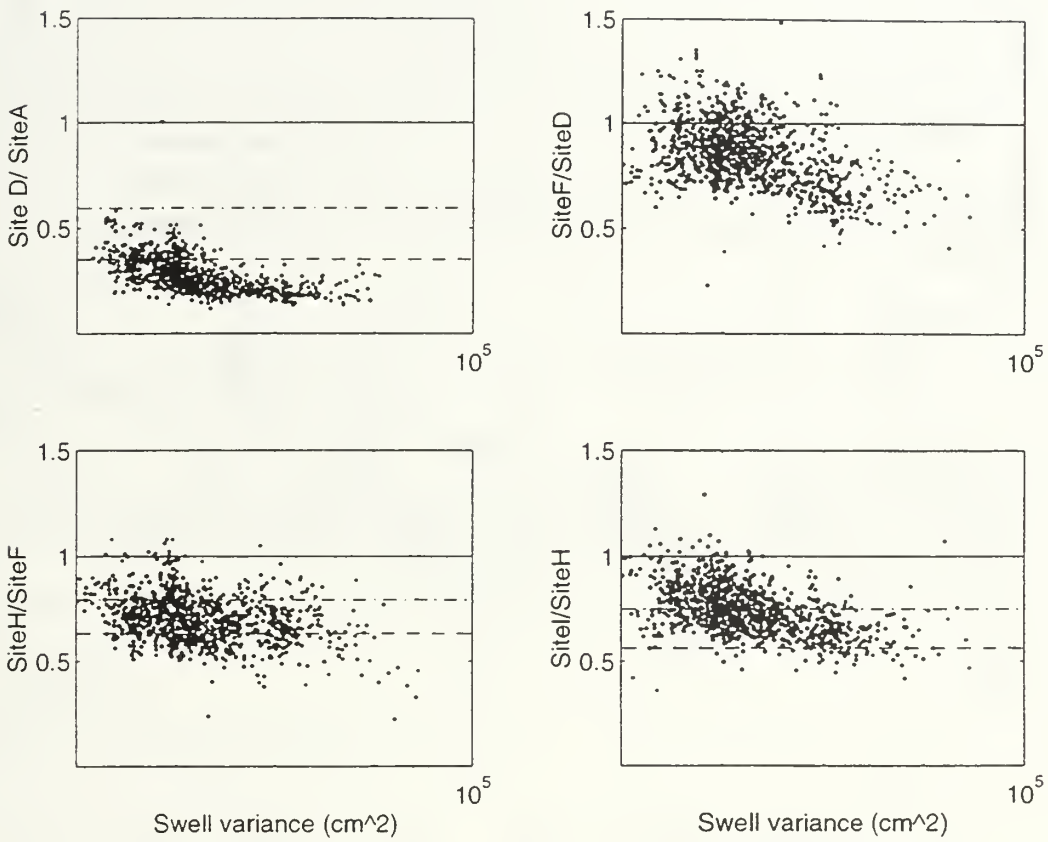
1.5
1
0.5
Site D/ SiteA
10^5
SiteF/SiteD
SiteH/SiteF
SiteI/SiteH
Swell variance (cm^2)

Figure 8

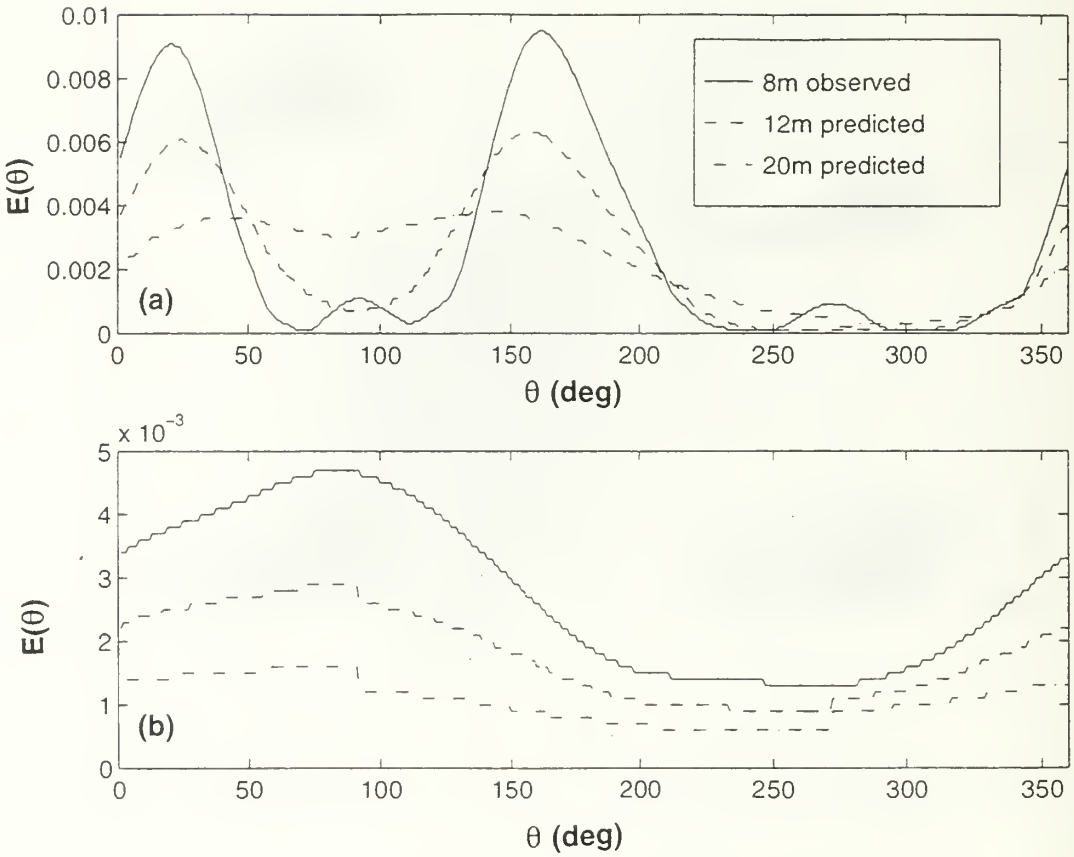
0.01
0.008
0.006
0.004
0.002
0
E(θ)
(a)
8m observed
12m predicted
20m predicted
0
50
100
150
200
250
300
350
θ (deg)
x 10^-3
5
4
3
2
1
0
E(θ)
(b)
0
50
100
150
200
250
300
350
θ (deg)

Figure 9

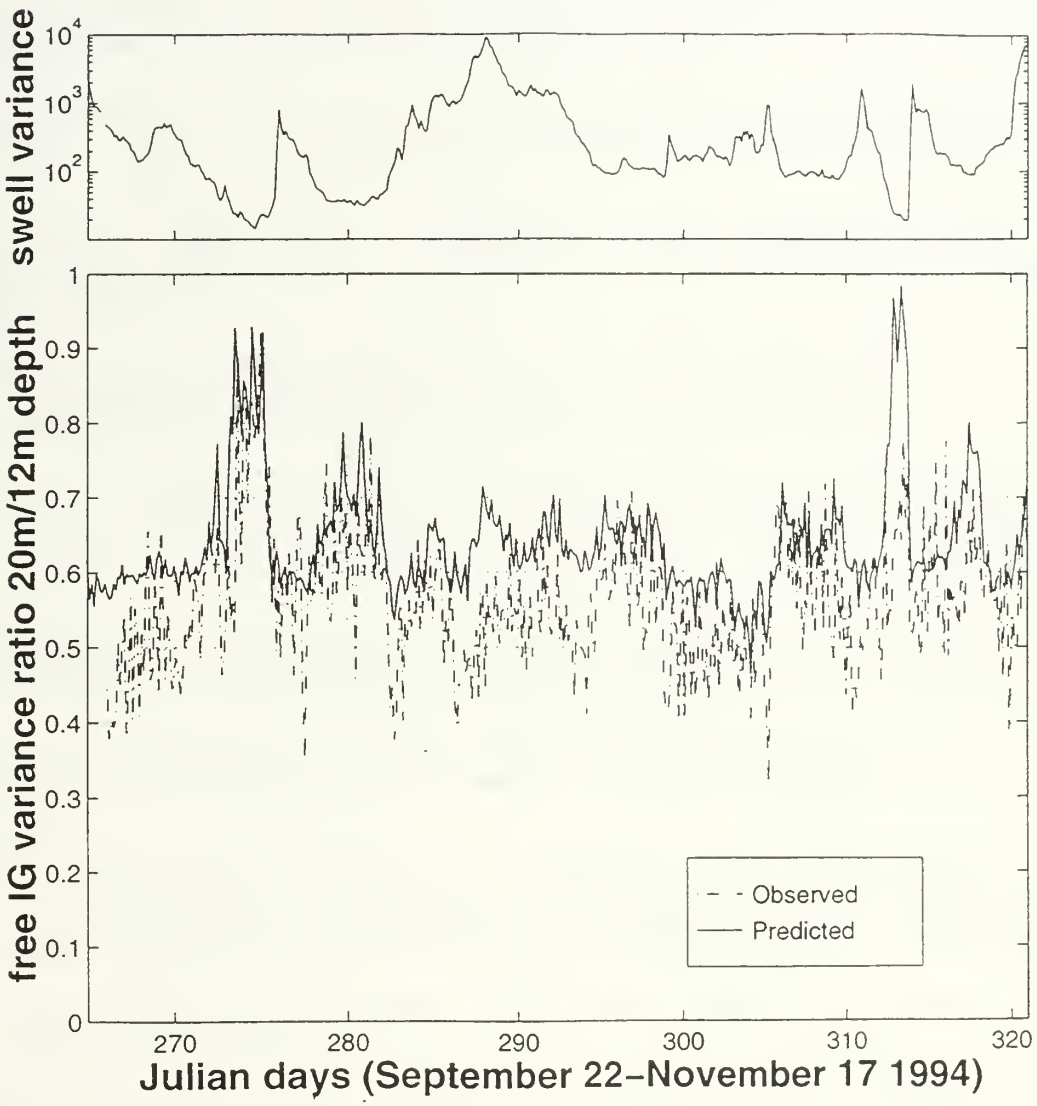
swell variance
10^4
10^3
10^2
free IG variance ratio 20m/12m depth
1
0.9
0.8
0.7
0.6
0.5
0.4
0.3
0.2
0.1
0
Observed
Predicted
270
280
290
300
310
320
Julian days (September 22–November 17 1994)

Figure 10

LIST OF REFERENCES

Elgar,S., T.H.C. Herbers, M. Okihiro, J. Oltman-Shay and R.T. Guza, 1992: Observations of infragravity waves. *J. Geophys. Res.*, 97, 15 573-15 577.

_____, _____ and R.T. Guza, 1994: Reflection of ocean surface gravity waves from a natural beach. *J.Phys.Oceanogr.*, 24, 1503-1511.

Hasselmann,K., 1962: On the nonlinear energy transfer in a gravity- wave spectrum. Part 1: General theory. *J.Fluid Mech.*,12,481-500.

_____, W. Munk, and G. MacDonald, 1963: Bispectra of ocean waves. *Time Series Analysis*, M. Rosenblatt, Ed., John Wiley, 125-139.

Herbers,T.H.C., and R.T. Guza, 1990: Estimation of directional wave spectra from multicomponent observations. *J.Phys.Oceanogr.*, 20, 1703-1724.

_____, S.Elgar and R.T.Guza, 1994: Infragravity-frequency (0.005-0.05 Hz) motions on the shelf. Part I: Forced waves. *J.Phys.Oceanogr.*, 24,917-927.

_____,_____,_____, and W.C. O'Reilly, 1995a infragravity frequency (0.005-0.5 Hz) motions on the shelf. Part II, Free waves, *J.Phys.Oceanogr.*, 25, 1063-1079.

_____,_____,_____, 1995b: Generation and propagation of infragravity waves, *J.Phys.Oceanogr.*, 24, 863-872.

Longuet-Higgins,M.S., and R.W. Stewart, 1962: Radiation stress and mass transport in surface gravity waves with application to "surf beats." *J.Fluid Mech.*,13, 481-504.

Munk,W.H., 1949: Surf beats. *EOS Trans. Amer. Geophys. Union*, 30, 849-854.

Okihiro, M., R.T. Guza, and R. J. Seymour, 1992: Bound infragravity waves. J. Geophys. Res., 97, 11 453-11 469.

Symonds, G., D.A. Huntley, and A. J. Bowen, 1982: Two dimensional surf beat: Long wave generation by a time varying break-point. J. Geophys. Res., 87, 492-498.

Tucker, M.J., 1950: Surf beats: Sea waves of 1 to 5 minute period. *Proc. Roy. Soc. London A*, 202, 565-573.

Webb, S.C., X. Zhang, and W. Crawford, 1991: Infragravity waves in the deep ocean. *J. Geophys. Res.*, 96, 2723-2736.

INITIAL DISTRIBUTION LIST

1.	Defense Technical Information Center 8725 John J Kingman Rd., STE 0944 Ft. Belvoir, VA 22060-6218	2
2.	Dudley Knox Library Naval Postgraduate School 411 Dyer Rd. Monterey, CA 93943-5101	2
3.	Dr. T.H.C. Herbers, Code Oc/He Department of Oceanography Naval Postgraduate School Monterey, CA 93943-5101	10
4.	Dr. E.B. Thornton, Code Oc/Tm Department of Oceanography Naval Postgraduate School Monterey, CA 93943-5121	1
5.	P.F. Jessen, Code Oc/Js Department of Oceanography Naval Postgraduate School Monterey, CA 93943-5121	1
6.	LT D.A. Evangelidis, H.N Hellenic Navy Hydrographic Service Stratopedo Papagou TGN 1040 Holargos ATHENS GREECE	3